Virus Research 356 (2025) 199578

Contents lists available at ScienceDirect

Virus Research

journal homepage: www.elsevier.com/locate/virusres

5,6-dihydroxyflavone exerts anti-betacoronavirus activity by blocking viral entry to host cells

Yujia Cao [a], Kah Man Lai [b], Hongling Zheng [a], Yee Joo Tan [b,*], Dejian Huang [a,c,*]

[a] Department of Food Science and Technology, National University of Singapore, Singapore 117542, Singapore
[b] Infectious Diseases Translational Research Program and Department of Microbiology and Immunology, Yong Loo Lin School of Medicine, National University of Singapore, Singapore 117545, Singapore
[c] National University of Singapore (Suzhou) Research Institute, 377 Linquan Street, Suzhou 215123, PR China

ARTICLE INFO

Keywords:
Anti-coronavirus
5,6-dihydroxyflavone
Receptor-binding domain
Flavones
Sars-cov-2

ABSTRACT

Baicalin, a bioactive flavone found in *Scutellaria baicalensis* Georgi has anti-SARS-CoV-2 infection by targeting viral 3C-like protease (3CLpro). However, little is known about the antiviral activity of its 7-deoxy analogue, 5,6-dihydroxyflavone (5,6-DHF), especially against betacoronaviruses (beta-CoVs). We found that 5,6-DHF exhibited more potent anti-SARS-CoV-2 Omicron variant EG.5.1.1 activity than baicalein by microneutralization test (MNT) and plaque reduction neutralization test (PRNT). 5,6-Dihydroxyl (catechol) groups at A ring of 5,6-DHF is essential for its suppression on SARS-CoV-2 Omicron variant EG.5.1.1 infection because blocking them with methyl or methylene groups obsolesce the activity. 3CLpro inhibition assay showed that the antiviral activity of 5,6-DHF is distinctive with baicalein. Time of addition test, molecular docking and spike-bearing pseudotyped virus entry assay suggested that 5,6-DHF interferes the spike-ACE2 interaction by targeting at receptor binding domain (RBD) of spike and hence inhibits the virus replication. In addition to SARS-CoV-2 Omicron variant EG.5.1.1, 5,6-DHF was also found effective against another common human beta-CoVs, HCoV-OC43, by blocking their entry to host cells. Taken together, the present study demonstrated the potential function of 5,6-DHF as a therapeutic candidate against beta-CoVs.

1. Introduction

Coronaviruses are enveloped, single-stranded, positive-sense RNA viruses that infect and spread between mammals and birds (Chang et al., 2020). Entering the twenty-first century, three highly pathogenic and deadly human coronaviruses (HCoV) including severe acute respiratory syndrome coronavirus (SARS-CoV), Middle East respiratory syndrome coronavirus (MERS-CoV) and severe acute respiratory syndrome coronavirus 2 (SARS-CoV-2) have emerged. Particularly, coronavirus disease 2019 (COVID-19) caused by SARS-CoV-2 has caused a devastating pandemic of acute respiratory disease, resulting in huge losses of human lives and economy (Zhu et al., 2020). As an RNA virus with high mutation rate, HCoV evolves rapidly from the wild-type virus to multiple variants of concerns (VOCs). These variants possess distinct phenotypic characteristics including elevated transmissibility, pathogenicity and immune evasion (Markov et al., 2023). Omicron variant with high transmissibility and immune evasion had emerged in November 2021 due to high number of mutations especially in the spike protein (Liu et al., 2024). Several Omicron subvariants like EG.5.1, FL.1.5.1 and XBB.1.1.16.6 had become the dominant strains globally and resulted in increased hospitalization and mortality in children or older people with comorbidities (da Silva, 2022).

Additionally, many other HCoVs such as HCoV-229E, HCoV-NL63 HCoV-OC43, and HCoV-HKU1 generally lead to epidemics with mild to moderate respiratory symptoms (He et al., 2020). According to the taxonomy of coronaviruses, SARS-CoV, SARS-CoV-2, MERS-CoV, HCoV-OC43 and HCoV-HKU1 are betacoronavirus, while HCoV-229E and HCoV-NL63 belong to alphacoronavirus (Yadav and Mohite, 2020). Currently, there is no specific treatment for HCoV infection. Several therapeutic agents, in the form of small molecular compounds or monoclonal antibodies (mAbs), with antiviral and immunomodulatory activity were candidates for curing COVID-19 (Drożdżal et al., 2021). Nonetheless, high cost, insufficient efficacy, immune evasion and unpredicted side effects limited their large-scale therapeutic application (Hashemian et al., 2023). Thus, there is urgent demand for the development of anti-betacoronavirus agents with low toxicity and high

* Corresponding authors.
E-mail addresses: mictyj@nus.edu.sg (Y.J. Tan), dejian@nus.edu.sg (D. Huang).

https://doi.org/10.1016/j.virusres.2025.199578
Received 11 August 2024; Received in revised form 9 April 2025; Accepted 22 April 2025
Available online 23 April 2025

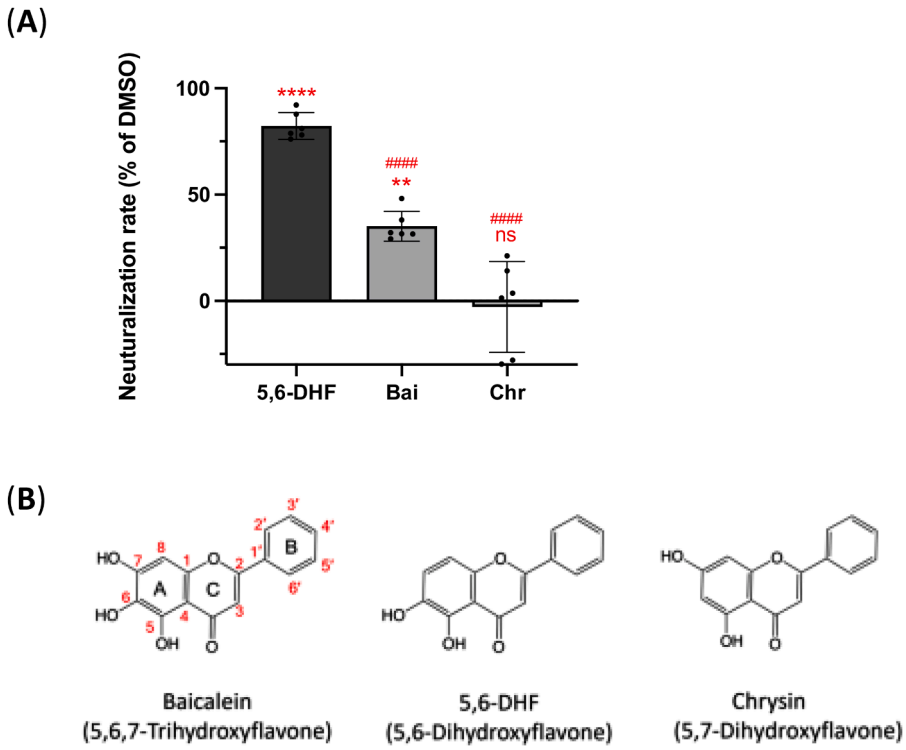

Fig. 1. Anti-SARS-CoV-2 Omicron variant EG.5.1.1 activity (**A**) and chemical structures (**B**) of 5,6-DHF, baicalein and chrysin. Antiviral activity of compound at 5 μM was evaluated using MNT. Data points and bar represent arithmetic shown are the mean ± SD of two independent tests performed. $^{**}P < 0.01$, $^{****}P < 0.0001$ as compared with DMSO group. $^{\#\#\#\#}P < 0.0001$ as compared with 5,6-DHF groups.

Table 1
Materials used in the research.

Materials	Manufacturers
5,6-dihydroxyflavone	Indofine Chemical Co., Inc (Hillsborough, NJ, US)
Chrysin (5,7-dihydroxyflavone, purity: 97 %),)	Shanghai Yien Chemical Technology Co., Ltd (Shanghai, China).
Baicalein (5,6,7-trihydroxyflavone, purity: 98 %), potassium carbonate, iodomethane (MeI), diiodomethane (CH_2I_2), dimethylformamide (DMF), Silica gel (230–400 mesh particle size), paraformaldehyde (PFA), tetramethylbenzidin (TMB), formalin solution, crystal violet, Nirmatrelvir (PF-07,321,332) and dimethyl sulfoxide (DMSO)	Sigma-Aldrich Co., Ltd. (Singapore).
3CL protease, MBP-tagged (SARS-CoV-2) assay kit (catalog #79,955–1)	BPS Bioscience Inc. (San Diego, CA, USA)
Anti-HCoV-OC43 nucleoprotein antibody, clone 542–7D (Cat. MAB9013)	MilliporeSigma (Singapore)
Horseradish peroxidase (HRP) conjugated secondary antibody	Thermo Fisher Scientific Co., Ltd. (Singapore)

therapeutic efficacy in preparation for the future.

Baicalein (Bai, Fig. 1**A**) is a natural flavone primarily exists in the root of *Scutellaria baicalensis* Georgi (Huangqin in Chinese) which is a traditional Chinese medicine (TCM) with broad biological and pharmacological activities (Zhao et al., 2019). It has been reported that baicalein showed anti-SARS-CoV-2 effect in Vero cells by targeting the viral 3-chymotrypsin-like protease (3CLpro) (Liu et al., 2021). The interaction of baicalein and SARS-CoV-2 3CLpro revealed by crystal structure suggested baicalein was a non-covalent, non-peptidomimetic inhibitors of SARS-CoV-2 3CLpro (Su et al., 2020). Also, baicalein significantly inhibited the replication of the SARS-CoV-2 in lung tissue and relieved the lung lesions caused by SARS-CoV-2 in hACE2 transgenic mice (Song et al., 2021). Previously, we found the number and position of hydroxyl group, especially the catechol group, strongly influence on the bioactivity of flavone aglycones (Wang et al., 2022). Moreover, there are flavones possessing one less OH groups than baicalein on A ring include 5,7-dihydroxyflavone (chrysin, Chr) and 5,6-dihydroxyflavone (5,6-DHF). They have been reported to be much less potent than baicalein in inhibiting SARS-CoV-2 3CLpro activity (Liu et al., 2021). However, their abilities to inhibit the replication of live SARS-CoV-2 have not been determined. In addition, molecular docking study demonstrated the binding of chrysin to the spike protein of SARS-CoV-2, suggesting its potential antiviral activity (Jantan et al., 2023). This difference between baicalein, 5,6-DHF and chrysin attracted our interest in finding impact of subtle chemical structural variations of flavonoids, especially the number and position of hydroxyl groups at the A ring, on their anti-coronavirus efficiency.

In this study, the antiviral activity of baicalein, 5,6-dihydroxyflavone and chrysin was evaluated against SARS-CoV-2 Omicron subvariant, EG.5.1.1 in vitro. Structure modification of flavones was conducted to further study the structure-activity relationship of flavones on the anti-coronavirus activity. The extensive anti-betacoronavirus activity of 5,6-dihydroxyflavone against HCoV-OC43 was also assessed.

2. Materials and methods

2.1. Materials

Materials used in the current study are listed in Table 1. 1A9 antibody with cross-reaction with SARS-CoV-2 spike protein was generated using spike protein on SARS-CoV (Lip et al., 2006; Zheng et al., 2020).

2.2. Synthesis of 5,6-DMF and 5,6-MDF

^{1}H and ^{13}C nuclear magnetic resonance spectroscopy (NMR) were conducted on Bruker AVANCE I 500 NMR spectrometer. NMR spectra

were collected by TopSpin 4.0.5 and analysed by MestReNova v12.0.0. Chemical shifts are recorded with solvent resonance as the internal standard: ^{1}H (DMSO-d_6: δ 2.50 ppm), ^{13}C (DMSO-d_6: δ 39.52 ppm). Data are reported as follows: chemical shift (δ ppm), integration, multiplicity (s = singlet, d = doublet, t = triplet, q = quartet, m = multiplet), and coupling constants (Hz). Thermo Scientific LCQ Fleet ion trap mass spectrometer or Waters Radian ASAP direct mass detector in electrospray positive and negative mode were employed. Reactions were monitored using thin layer chromatography (TLC).

The synthesis of 5,6-dimethoxyflavone (5,6-DMF) was carried out based on precious method with slight modification (Wang et al., 2011). 5,6-dihydroxyflavone (20.0 mg, 0.0787 mmol, 1 eq), K_2CO_3 (27.2 mg, 0.1969 mmol, 2.5 eq), and MeI (85.8 mg, 0.6058 mmol, 7 eq) were dissolved in dimethylformamide (DMF, 1.5 mL). The reaction mixture was then heated under reflux at 60 °C for 8 h. Afterward, the solvent was evaporated under reduced pressure, and the resulting residue was purified using silica gel chromatography, yielding the methylated product as a yellow solid (3.3 mg, 15 % yield). ^{1}H NMR (500 MHz, DMSO-*d6*): δ 8.07 (dd, J = 7.0, 2.1 Hz, 2H), 7.64 – 7.50 (m, 5H), 6.84 (s, 1H), 3.87 (s, 3H), 3.77 (s, 3H); ^{13}C NMR (126 MHz, DMSO-d_6): δ 176.89, 160.88, 150.67, 149.77, 146.49, 131.77, 131.04, 129.22 (2C), 126.26 (2C), 119.38, 118.53, 113.98, 107.25, 61.20, 56.66. HRMS (ESI-TOF) calcd for $C_{17}O_4H_{14}Na$ $[M+Na]^+$ = 305.0784, found at 305.0789.

The synthesis of 5,6-methylenedioxyflavone (5,6-MDF) was carried out based on a precious method with slight modification (Wang et al., 2011). 5,6- Dihydroxyflavone (20.0 mg, 0.0787 mmol), K_2CO_3 (27.2 mg, 0.1969 mmol, 2.5 eq), and CH_2I_2 (15.88 μL, 0.1969 mmol, 2.5 eq) were dissolved in DMF (1.5 mL). The reaction mixture was stirred for 5 h at room temperature and diluted with dichloromethane (DCM), and then washed with diluted HCl and brine sequentially. The organic phase was concentrated in vacuo and the crude product was further purified by silica gel chromatography to afford the pure product as white solid (3.8 mg, 18 % yield). ^{1}H NMR (500 MHz, DMSO-d_6): δ 8.04 (dd, J = 7.5, 1.5 Hz, 2H), 7.58 (m, 3H), 7.37 (d, J = 8.7 Hz, 1H), 7.24 (d, J = 8.6 Hz, 1H), 6.85 (s, 1H), 6.22 (s, 2H); ^{13}C NMR (126 MHz, DMSO-d_6): δ 176.33, 162.61, 150.65, 144.69, 144.65, 132.12, 131.16, 129.39 (2C), 126.51 (2C), 113.76, 110.53, 110.28, 106.41, 103.44. HRMS (ESI-TOF) calcd for $C_{16}O_4H_{10}Na$ $[M+Na]^+$ = 289.0471, found at 289.0475.

2.3. Cells and viruses

Vero E6 cells and H1299 were obtained from the American Type Culture Collection (ATCC) and cultured in Dulbecco's modified eagle medium (DMEM, Cytiva) with 10 % fetal bovine serum (FBS) and 1 % non-essential amino acid (NEAA, Thermo Fisher Scientific). CHO cell line stably expressing the human ACE2 (CHO-ACE2) was established previously (Lip et al., 2006). All cell lines were maintained in the humidified incubator with 5 % CO_2 at 37 °C. HCoV-OC43 was obtained from ATCC while SARS-CoV-2 Omicron variant EG.5.1.1 was patient-derived and propagated in Vero E6 cell (hCoV-19/Singapore/NUS0001/2023, GISAID accession: *EPI*_ISL_19,016,298).

2.4. Cell cytotoxicity

H1299 cells, Vero E6 cells and CHO cells were seeded in a 96-well plate and incubated until the wells were filled with a monolayer of cells. After finishing the treatment with samples, cell viability was measured using CCK-8 assay kit (Dojindo Molecular Technologies, Inc., Japan) according to manufacturer's instructions. The absorbance at 450 nm was measured with the Tecan Spark multimode microplate reader. Cell viability was calculated as compared to the untreated group.

2.5. Microneutralization test (MNT)

Virus was pre-titrated in plaque-forming units (PFU) by plaque assays before testing. Vero E6 cells and H1299 cells were seeded in 96-well plate and incubated overnight. A mixture of virus inoculum at the multiplicity of infection (MOI) of 0.025 to 0.1 and samples was prepared for cell infection. The same amount of DMEM was topped up after 1 h of virus absorption in 37 °C. After incubating for another 23 h, cells were fixed with 4 % PFA, permeabilized with 0.2 % Triton-X-100 (BDH, USA), and blocked with 10 % FBS in phosphate-buffered saline (PBS, Bio Basic Asia Pacific Pte. Ltd.). Anti-SARS-CoV spike 1A9 antibody, and HRP-linked secondary antibody was then incubated with cells. TMB substrate was applied to visualize the enzymic reaction and it was ceased after 5 min with 1 M sulfuric acid. The absorbance at 450 nm was measured by Tecan Spark multimode microplate reader. The calculation for neutralization rate was based on previous report (Amanat et al., 2020).

$$\text{Neutralization rate} = 100\% - \left(A_{sample} - A_{mock}\right)/\left(A_{DMSO} - A_{mock}\right) \times 100\%$$

where A_{mock}, A_{DMSO} and A_{sample} represent the absorbance of the non-infected, DMSO treated and sample tested group at 450 nm, respectively.

2.6. Plaque reduction neutralization test (PRNT)

H1299 cells and Vero E6 cells were seeded in a 12-well plate and incubated overnight for cells to form a monolayer. The mixture of indicated virus inoculum (160 to 200 PFU/mL) and sample at indicated concentration was incubated with designed wells. To improve the virus adsorption, cells were incubated in 37 °C humidified incubator for 1 h with gently rocked every 10 min. After that, the mixture containing unabsorbed virus was replaced with the same concentration of samples diluted using overlay (1 % FBS in minimum essential medium (MEM, Thermo Fisher Scientific) and 1.2 % Avicel (FMC BioPolymer, USA)). At the 3 days post infection (dpi), cells were fixed with 10 % formalin and stained with 0.1 % crystal violet. The neutralization rate was calculated with reference to reported work (Liu et al., 2012).

$$\text{Neutralization rate} = 100\% \times \left[1 - \left(N_{sample} / N_{DMSO}\right)\right]$$

where N_{DMSO} and N_{sample} represent the average number of plaques in the DMSO treated and sample tested group, respectively.

2.7. 3CL protease inhibitory assay

3CL protease MBP-tagged (SARS-CoV-2) assay kit was used to study the inhibition of 3CLpro according to manufacturer's recommended procedure. Nirmatrelvir was included as inhibitor control. Briefly, 100 μM flavones and nirmatrelvir were prepared in an assay buffer containing 1 mM dithiothreitol (DTT) and preincubated with 70 ng 3CLpro at room temperature for 30 min with gentle shaking. The positive control was the reaction mixture with DMSO in place of inhibitors. The reaction was initiated by adding fluorogenic 3CL protease substrate (25 μM), and the sealed plate was incubated overnight. The fluorescence intensity was measured by BioTek Cytation 5 Cell Imaging Multimode Reader at the excitation and emission wavelengths of 360 nm and 460 nm, respectively. The percentage of inhibitory activity was calculated using the following equation:

$$\%\ \text{Activity} = 100\% - \left(F_{sample} - - F_{blank}\right)/\left(F_{positive} - F_{blank}\right) \times 100\%$$

Where F_{blank}, $F_{positive}$ and F_{sample} represent the fluorescence intensity of the blank, positive control and sample tested group, respectively.

2.8. Molecular docking

The 3D structure of 5,6-DHF (CID: 14,349,487) were downloaded in SDF format from PubChem. The Autodock vina was employed for the molecular docking study. Hydrogen atoms were added and unnecessary

Table 2
Anti-SARS-CoV-2 Omicron variant EG.5.1.1 properties and cytotoxicity of 5,6-DHF, baicalein and nirmatrelvir.

Compounds	IC_{50} (μM)	CC_{50}(μM)	SI
5,6-DHF	1.716 ± 0.2830	> 50	> 29.14
Baicalein	5.570 ± 0.2650	> 50	> 8.977
Nirmatrelvir	0.6838 ± 0.0955	> 50	> 73.12

Selectivity index (SI) was calculated as the ratio of the CC_{50} against its IC_{50}. Data shown are the mean ± SD of two independent tests performed.

water molecules were removed before docking. The crystal structure of SARS-CoV-2 receptor-binding domain (RBD) (7RBY) was obtained from the Protein Data Bank (http://www.rcsb.org/pdb/). The top binding poses with the highest binding energy in the binding pocket were reported. The images were generated using PyMol 2.5.5.

2.9. Time of addition assay

Vero E6 and H1299 cells were seeded in a 96-well plate and incubated overnight for cells to form a monolayer. The cell was infected with SARS-CoV-2 (MOI = 0.025), HCoV-OC43 (MOI = 0.1) and treated with 5,6-DHF (5 μM for Vero E6 cells and 12.5 μM for H1299 cells) at indicated timepoints. In standard treatment, virus and 5,6-DHF was added simultaneous into the cell and incubated for 1 h followed by addition of 50 μL media. In pre-treatment, cells were pre-treated with 5,6-DHF for 1 h and the inoculum was removed prior virus infection. In co-treatment, virus and 5,6-DHF were mixed and incubated for 1 h prior addition into the cells. For post-treatment, cell was infected with virus for 1 h followed by addition of 5,6-DHF. Except for standard treatment, virus inoculum with or without 5,6-DHF were removed after 1 h of virus adsorption and cells were replenished with fresh medium. After 24 h of incubation, cell was fixed with 4 % PFA and subjected to MNT.

2.10. SARS-CoV-2 spike pseudotyped virus entry assay

SARS-CoV-2 spike pseudotyped virus was generated by co-transfection of a plasmid encoding the envelop-deficient HIV-1 NL4–3 virus with luciferase reporter gene (pNL4–3.Luc.R-E-) and a pTT5 plasmid expressing the SARS-CoV-2 spike protein, which contains a 19 amino acid C-terminal truncation, into HEK 293FT cell using X-tremeGENE 360 transfection reagent (Roche) (Lam et al., 2021). After 48 h of incubation, culture supernatant was collected and the pseudotyped virus produced was titered using QuickTiter™ Lentivirus Titer Kit (Cell Biolabs) according to the manufacturer's protocol. For entry assay, CHO-ACE2 cell was seeded at 1.8×10^4 cell/well in white flat bottom 96-well plate and cultured overnight. 0.125 ng/mL of spike-bearing pseudotyped virus was incubated with 5,6-DHF at indicated concentration for 1 h at RT. The mixture was added to the cell and incubated for 48 h. Luciferase activity of infected cells in relative light units (RLU) was measured using Bright-Glo™ Luciferase Assay System (Promega) according to the manufacturer's instruction.

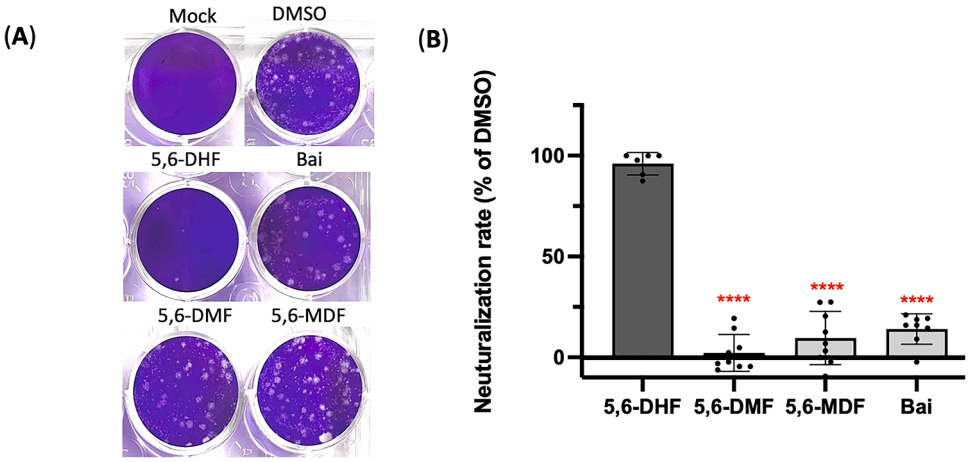

Fig. 2. PRNT of 5,6-DHF and its structural analogue against SARS-CoV-2 Omicron variant EG.5.1.1 infection at the concentration of 1 μM (**A**). Neutralization rate of PRNT was plotted (**B**). Data points and bar represent arithmetic shown are the mean ± SD of two independent tests performed. $^{****}P < 0.0001$ as compared with 5,6-DHF groups.

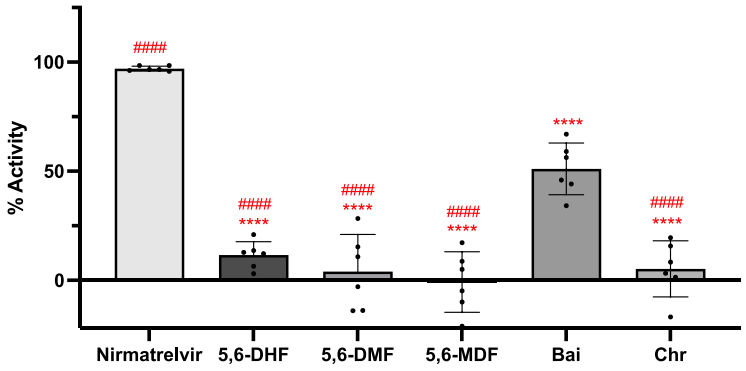

Fig. 3. Inhibitory activity of selected flavones on SARS-CoV-2 3CLpro. The activity was tested with the compound concentration of 100 μM. Data points and bar represent arithmetic shown are the mean ± SD of at least two independent tests performed. $^{****}P < 0.0001$ as compared with nirmatrelvir group, $^{\#\#\#\#}P < 0.0001$ as compared with baicalein groups.

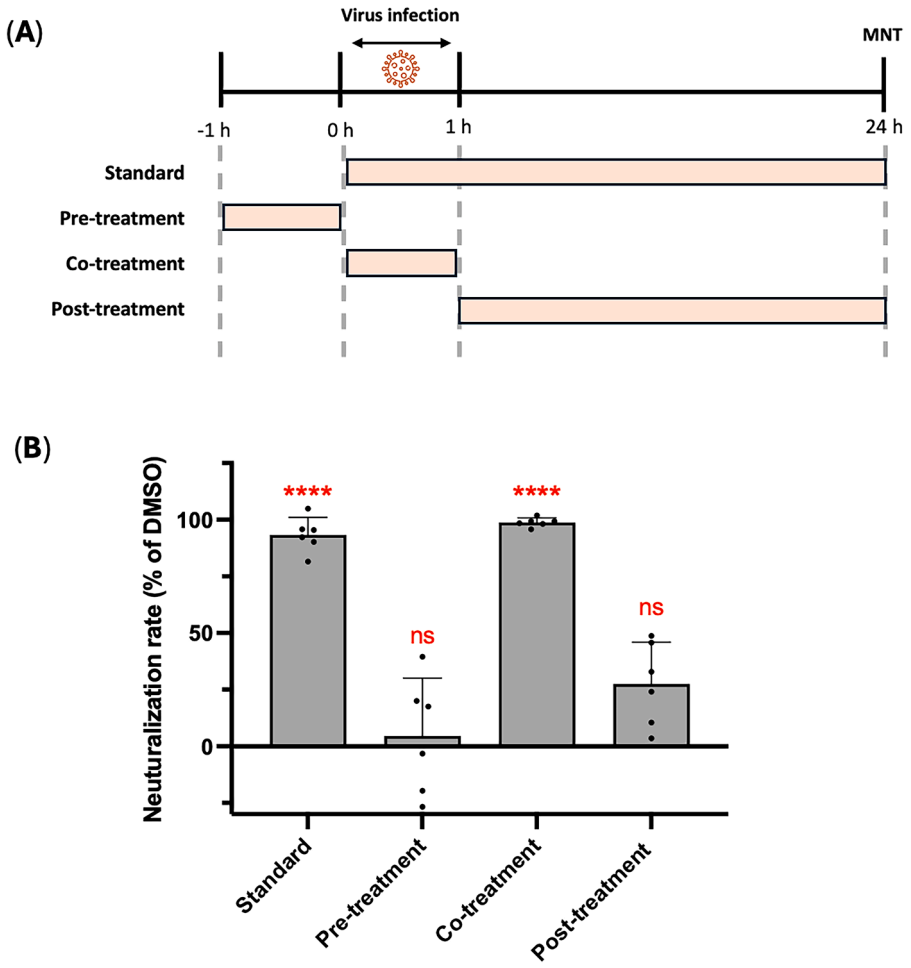

Fig. 4. Time of addition assay of 5,6-DHF against SARS-CoV-2. Schematic presentation of time of addition assay (**A**). Antiviral activity of 5,6-DHF at different timepoints was evaluated using MNT and the neutralization rate was plotted (**B**). Data points and bar represent arithmetic shown are the mean ± SD of three independent tests performed. ****$P < 0.0001$ as compared with corresponding DMSO treatment.

2.11. Viral replication kinetics

H1299 cells were infected with the HCoV-OC43 at the MOI of 0.01 with DMSO or 5 μM 5,6-DHF. After incubation at 37 °C for 1 h, the inoculum was replaced with fresh medium with DMSO or 5 μM 5,6-DHF. Cell were then incubated at 37 °C and culture supernatants were collected at 1, 2, 3, 4 and 5 days post-infection and fresh DMSO or 5 μM 5,6-DHF were replenished every day. Virus titers were determined by plaque assay in H1299 cells.

2.12. Statistical analysis

Statistical analysis of the data was done by GraphPad Prism (version 9.5.0). Multi-group data comparisons were analysed by Student's *t*-test, one-way analysis of variance (ANOVA) or two-way ANOVA. *$P < 0.05$ was considered statistically significant. The codes of analysis are listed in the **Table S2**.

3. Results

3.1. Anti-SARS-CoV-2 properties of selected flavones

Anti-SARS-CoV-2 activity of selected flavones was evaluated using MNT. At the concentration of 5 μM, baicalein and 5,6-DHF exerted 35.12 % and 82.32 % of neutralization rate against SARS-CoV-2 Omicron variant EG.5.1.1 infection in Vero-E6 cell respectively. Whereas, chrysin did not neutralize SARS-CoV-2 Omicron variant EG.5.1.1 infection (Fig. 1**A**). This finding suggested that the existence of 7-hydroxyl group in baicalein attenuated its antiviral activity, while 5,6-dihydroxyl group at A ring in 5,6-DHF was crucial for the anti-SARS-CoV-2 effect (Fig. 1**B**). As baicalein were reported to have inhibitory effect against SARS-CoV-2 3CLpro, their antiviral potency was compared with nirmatrelvir which has been approved for the treatment of mild-to-moderate COVID-2019 as SARS-CoV-2 3CLpro inhibitor (Hashemian et al., 2023). The half-maximal inhibitory concentration (IC_{50}) against SARS-CoV-2 Omicron variant EG.5.1.1, 50 % cytotoxic concentration (CC_{50}) on Vero E6 cells and selective index (SI) were summarized in Table 2. The IC_{50} of 5, 6-DHF was about 3 times lower than that of baicalein, indicating much high potency of 5,6-DHF on SARS-CoV-2 Omicron variant neutralization. Additionally, though baicalein could inhibit SARS-CoV-2 3CLpro shown on a resolved crystal structure, its anti-SARS-CoV-2 activity was much inferior to nirmatrelvir.

According to previous research, the methylation of hydroxyl groups on flavones could improve their biological effects (Walle, 2009). With the aim to further improve the function of 5,6-dihydroxyl group on the neutralization of SARS-CoV-2 Omicron variant EG.5.1.1, we modified the structure of 5,6-DHF to 5,6-DMF and 5,6-MDF. Their chemical structures characterized by nuclear magnetic resonance (NMR) were showed in **Fig S1 & S2**. The anti-SARS-CoV-2 activity was measured by plaque reduction neutralization test (PRNT) against SARS-CoV-2 Omicron variant EG.5.1.1. The cytotoxicity of flavones at tested concentration on Vero E6 cells was negligible (**Fig. S3**). Among all tested

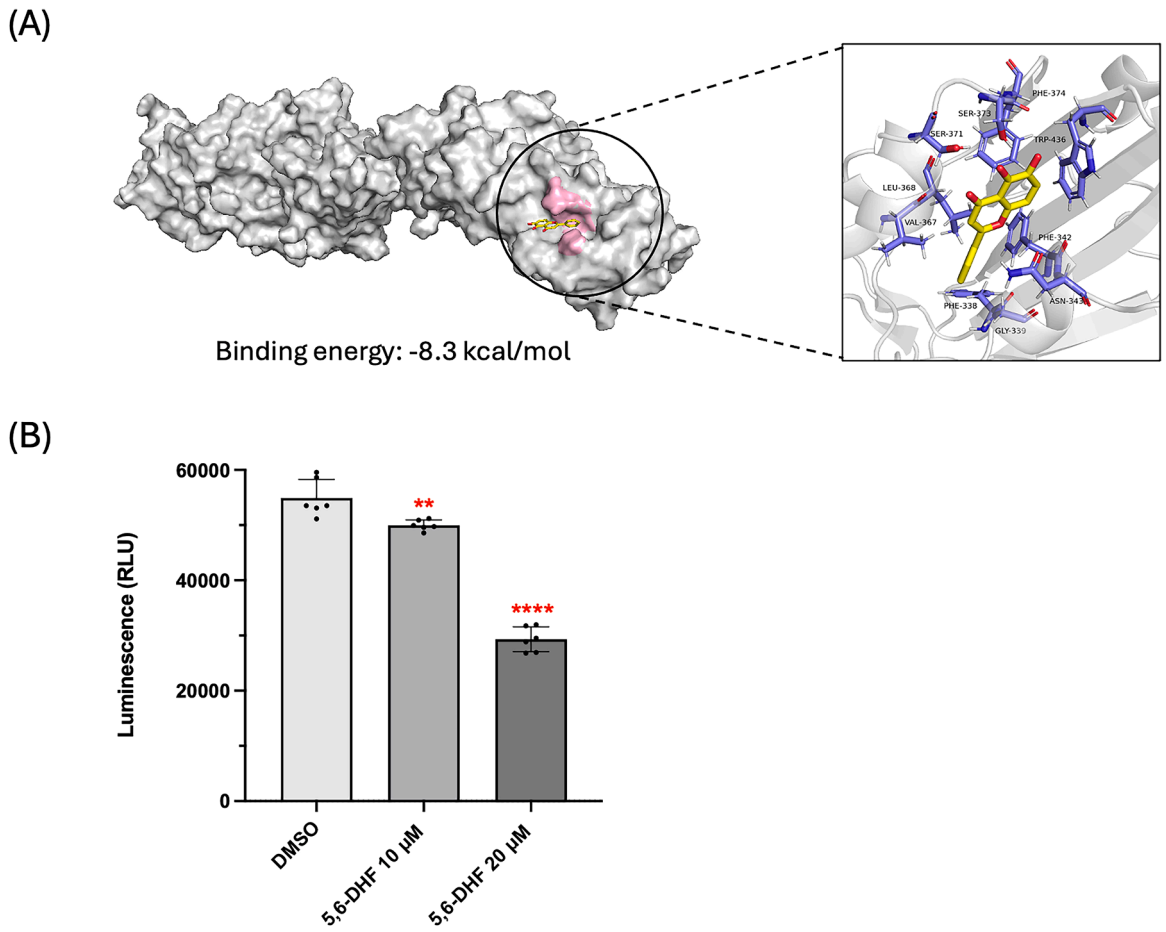

Fig. 5. Molecular docking of 5,6-DHF with RBD of SARS-CoV-2 wildtype strain (PDBID: 7RBY) and its potential neighbor amino acid residues (**A**). Inhibitory activity of 5,6-DHF on the entry of spike-bearing pseudotyped virus on ACE2 expressing CHO cells (**B**). Data points and bar represent arithmetic shown are the mean ± SD. $^{**}P < 0.01$ $^{****}P < 0.0001$ as compared with DMSO group.

structural analogues, 5,6-DHF showed the most potent anti-SARS-CoV-2 Omicron variant EG.5.1.1 activity (Fig. 2). This result further supported the important role of 5,6-dihydroxyl group played in the SARS-CoV-2 neutralization process. Consistent with MNT (Fig. 1**A**), PRNT confirmed that the antiviral activity of 5,6-DHF is higher than Bai (Fig. 2).

3.2. Inhibitory activity of SARS-CoV-2 3CLpro

Previous studies have reported the non-covalent, non-peptidomimetic inhibition of baicalein on the SARS-CoV-2 3CLpro. As compared to baicalein, 5,6-DHF showed lower inhibitory effect (Liu et al. 2021 We tested their inhibitory activity of the flavones on SARS-CoV-2 3CLpro with nirmatrelvir as positive control (Fig. 3) and found they did not exert inhibitory effects on SARS-CoV-2 3CLpro as nirmatrelvir (Fig. 3). All of flavones tested did not exert the same vigorous inhibitory effects on SARS-CoV-2 3CLpro as nirmatrelvir. Remarkably, baicalein showed significant higher suppression on SARS-CoV-2 3CLpro as compared with 5,6-DHF, 5,6-MDF, 5,6-DMF and chrysin, which confirmed the anti-SARS-CoV-2 effects of baicalein was mainly due to its function on SARS-CoV-2 3CLpro. Additionally, this result suggested that the more potent anti-SARS-CoV-2 activity of 5,6-DHF might involve different mechanism(s) of action than that of baicalein.

3.3. 5,6-DHF inhibit viral entry of SARS-CoV-2 infection by targeting spike protein

Time of addition assay was conducted to identify the mechanism of inhibitory effect of 5,6-DHF against SARS-CoV-2 Omicron variant EG.5.1.1 infection. Standard treatment and co-treatment of virus with 5,6-DHF significantly inhibited SARS-CoV-2 infection (Fig. 4). In contrast, pre-treatment and post treatment with 5,6-DHF did not inhibit virus infection (Fig. 4). These findings indicated that 5,6-DHF targeted entry stage of virus infection and its inhibitory activity did not involve host receptor and cellular regulation.

As the time of addition assay indicated that 5,6-DHF mainly participated in the entry stage of SARS-CoV-2 infection, we proposed that it targeted the spike protein of SARS-CoV-2. Molecular docking suggested that 5,6-DHF could bind RBD of SARS-CoV-2 wildtype strain at the active binding pocket with binding energy of −8.3 kcal/mol (Fig. 5**A**). Baicalein failed to be docked into that active binding pocket with the top ten proposed binding poses. And chrysin exhibited much lower binding affinity compared with 5,6-DHF (**Fig. S4**). To further understand the interaction of 5,6-DHF with SARS-CoV-2 spike protein, entry assay of pseudotyped virus carrying spike protein of SARS-CoV-2 wildtype strain in CHO-ACE2 cell was conducted. 5,6-DHF at concentration of 25 μM and below did not affect the cell viability (**Fig. S5**). Pre-incubation of pseudotyped virus with 10 μM and 20 μM of 5,6-DHF significantly reduced the luciferase activity with 8.96 % and 46.62 % of reduction in RLU as compared to control, respectively (Fig. 5**B**). This indicated that 5,6-DHF was able to interfere the spike-ACE2 interaction by targeting RBD and prevented the entry of virus, therefore inhibiting the replication of SARS-CoV-2 in host cells (Fig. 6).

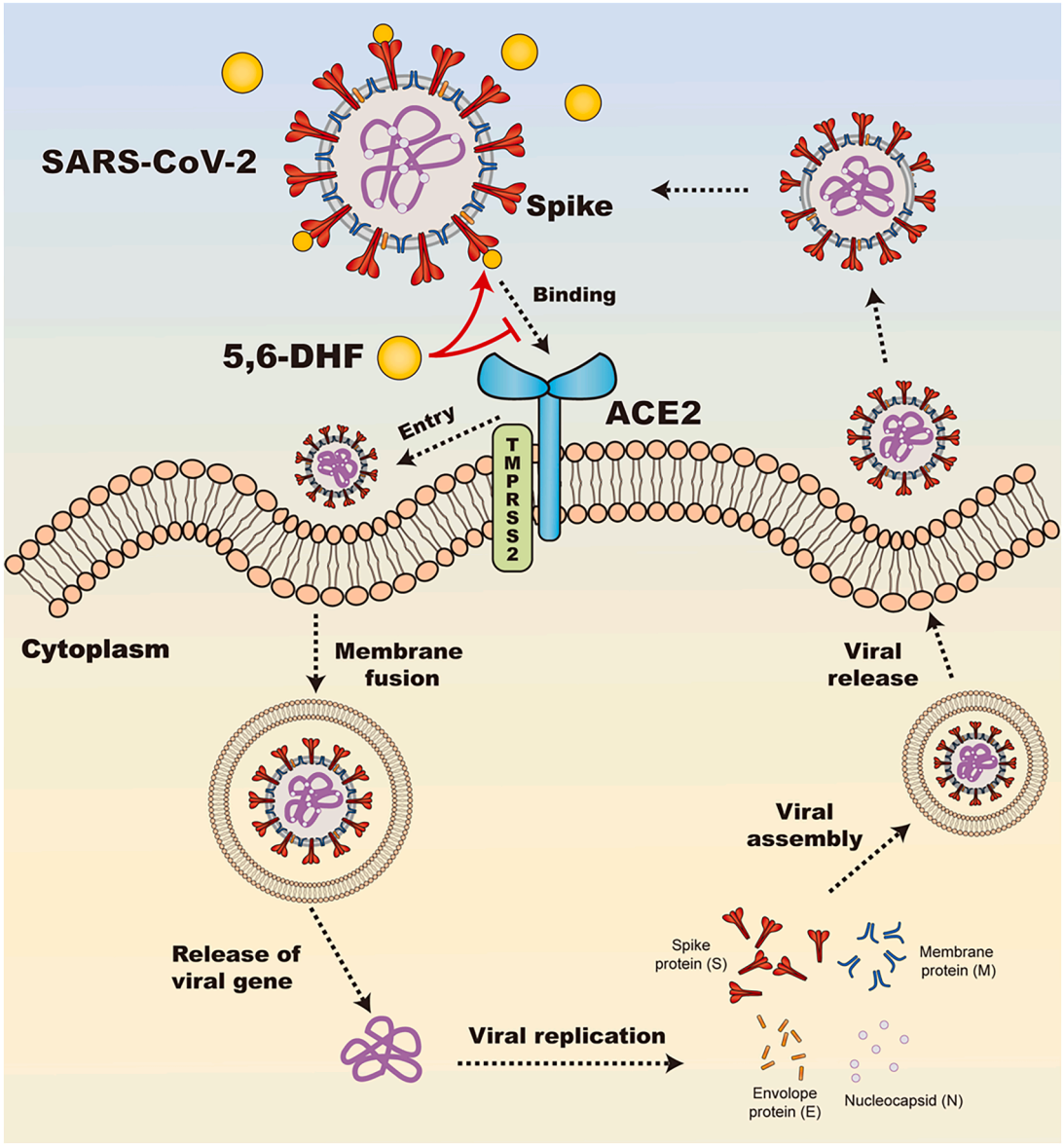

Fig. 6. Proposed antiviral mechanism of 5,6-DHF on SARS-CoV-2 replication process by blocking the binding of the virus with host cell receptor.

3.4. 5,6-DHF exhibits anti-betacoronavirus activity against HCoV-OC43

To determine the anti-coronavirus activity of 5,6-DHF against other beta-CoVs, it was evaluated on H1299 cells against beta-coronavirus HCoV-OC43 using PRNT. We observed 5,6-DHF could significantly neutralize HCoV-OC43 infection at 0.5 μM, while the SARS-CoV-2 3CLpro inhibitor baicalein was unable to inhibit the replication of HCoV-OC43 even at 1 μM (Fig. 7**A-B**). In agreement with previous studies, nirmatrelvir exerted antiviral activity against seasonal HCoVs (Li et al., 2023), and baicalein failed to exhibit its potency against HCoV-OC43 at low concentrations (Mori et al., 2023) (Fig. 7**A-B**). Additionally, MNT results indicated 5,6-DHF could neutralize HCoV-OC43 with the IC_{50} of 1.355 ± 0.1730 μM (Fig. 7**C**). The potential mechanism by which 5,6-DHF neutralized HCoV-OC43 was clarified by the time of addition assay. Standard, co-treatment and post-treatment of 5,6-DHF showed significantly inhibition on viral replication, importantly, the inhibitory rate of co-treatment was significantly greater than pre-treatment and post treatment, suggesting the principal function of 5,6-DHF on blocking HCoV-OC43 entry to host cells (Fig. 7**D**). The HCoV-OC43 growth kinetic activity and long-term anti-HCoV-OC43 activity of 5,6-DHF was also evaluated at the condition where 5,6-DHF did not show cytotoxicity to H1299 cells (**Fig. S6**). HCoV-OC43 replicated dramatically after infection, but 5,6-DHF could inhibit the replication of HCoV-OC43 in H1299 cells for at least 5 dpi (Fig. 7**E**).

4. Discussion

The perpetual emergence of new variants of SARS-CoV-2 with increased transmissibility and resistance to current treatments or vaccine has raised concerns. It is crucial to develop novel anti-SARS-CoV-2 agents to negate the resistant variants. Flavonoids have been received extensively interest as therapeutic agents against coronavirus because of their documented anti-viral, low toxicity and anti-inflammatory activities (Kaul et al., 2021). Several studies have reported that flavonoids exhibit inhibitory effect on SARS-CoV-2 replication by interacting with multiple targets and stages of viral life cycle, including inhibition of spike-ACE2, viral RNA-dependent RNA polymerase (RdRp), non-structural protein-15 (Nsp-15) as well as 3CLpro (Yang et al., 2023).

Comparison of anti-SARS-CoV-2 activity of tested flavones revealed that the importance of 5,6-dihydroxyl group in the suppressive function

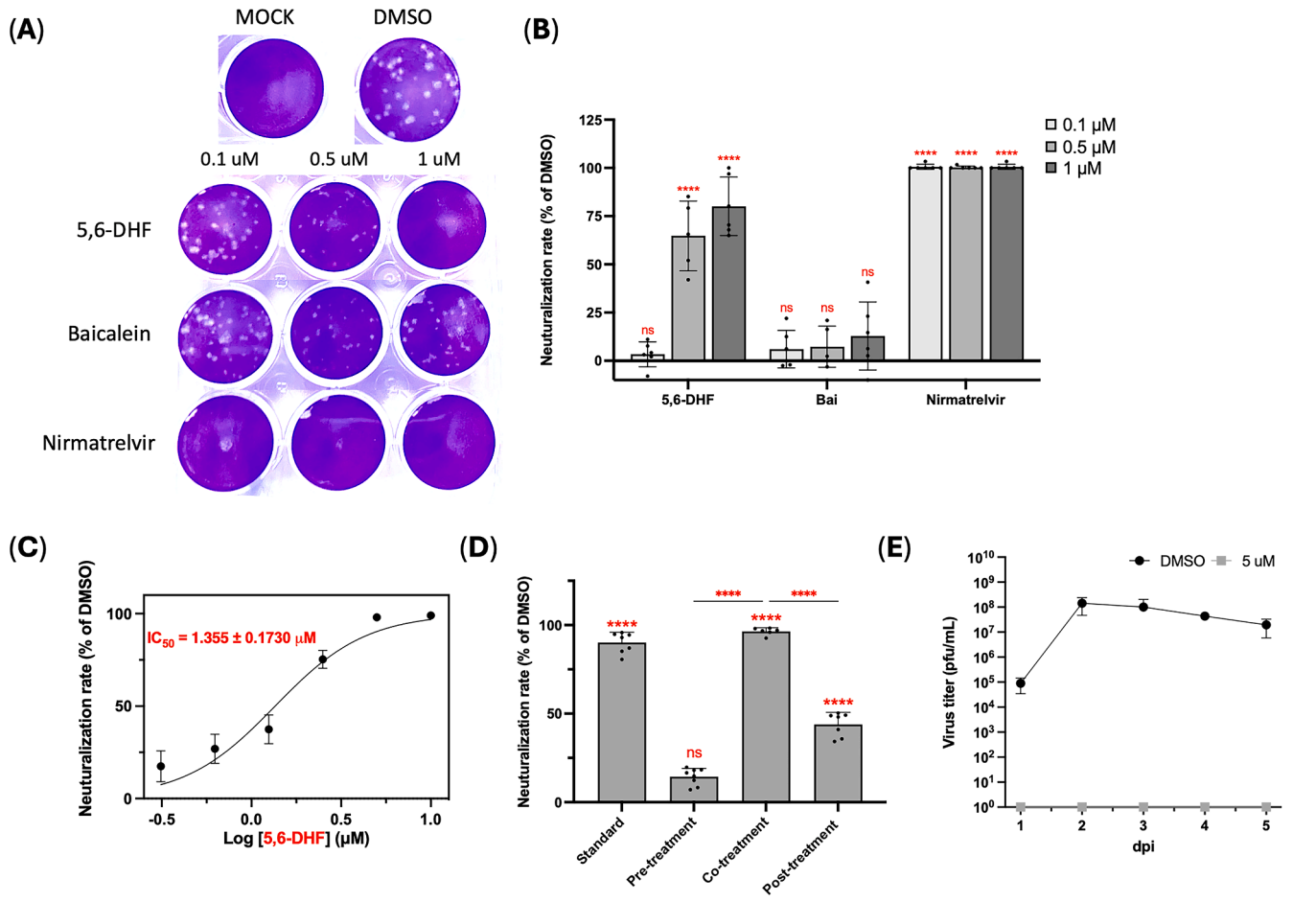

Fig. 7. PRNT of flavones and nirmatrelvir against HCoV-OC43 (**A, B**). IC_{50} of 5,6-DHF (**C**) and time of addition results of 5,6-DHF (**D**) against HCoV-OC43 determined by MNT. (**E**) HCoV-OC43 growth kinetic in H1299 cells with the DMSO or 5 μM 5,6-DHF. Data points and bar represent arithmetic shown are the mean ± SD. ****$P < 0.0001$ as compared with corresponding DMSO group or between indicated groups.

on SARS-CoV-2 infection. This is further supported by the chemical modification on 5,6-DHF which eradicated the antiviral activity. On the other hand, 3CL protease inhibitory assay and time of addition assay suggested that 5,6-DHF exerted antiviral activity through a mechanism distinctive from baicalein. Molecular docking and spike-bearing pseudotyped virus entry assay revealed that 5,6-DHF could interrupt spike-ACE2 interaction by binding to RBD and hence prevent viral entry. The anti-coronavirus activity of 5,6-DHF was not restricted to SARS-CoV-2 Omicron variant EG.5.1.1, but also extended to other human pathogenic coronaviruses HCoV-OC43 which could cause more severe illness in immunocompromised, young and elderly populations. Remarkably, HCoV-OC43 was employed as effective surrogate virus for SARS-CoV-2 research as they shared similar properties (Song et al., 2021). Further investigation revealed 5,6-DHF also predominantly targeted at the entry stage of viral replication.

Viral life cycle of SARS-CoV-2 consists of five stages including viral entry, viral genome translation, subgenomic transcription, genome replication and progeny virion formation. Viral entry is the key step in the initiation of viral life cycle and serves as an ideal target for antiviral treatment. It has been reported that post-exposure prophylaxis effectively prevents illness following potential or confirmed exposure to various microbial pathogens and facilitate to suppress the risk of infection transmission (Bader and McKINSEY, 2013). Clinical trials have demonstrated that post-exposure prophylaxis with antiviral agents is effective in preventing SARS-CoV-2 infection and minimizing the risk of developing COVID-19 infection related symptoms and death (Shmuelian et al., 2023; Wischmeyer et al., 2024). A number of therapeutic mAbs that target RBD have been developed for the post-exposure prophylaxis, however, the rise of resistant Omicron subvariants has limited the effectiveness and lead to withdrawal of these mAbs. Spike-targeting small molecules and natural compounds including flavones that have better pharmacokinetics, stability and dosage logistics could be an alternative approach in counteracting new emerging variants (Dong et al., 2024). In addition, immunomodulatory and anti-inflammatory properties of flavones are well described and could potentially be employed in the treatment of complicated COVID-19 symptoms associated with exaggerated immune responses (Alzaabi et al., 2022; Liskova et al., 2021). However, due to limited research, few flavonoids have been advanced to the clinical stage.

Taken together, the present study reported the potent anti-beta-CoVs activity of 5,6-DHF and its underlying mechanism of action. However, further investigation on the anti-inflammatory and immunomodulatory properties of 5,6-DHF is needed to elucidate the potential application of 5,6-DHF in modulating beta-CoV-induced immune response. In addition, numerous mutations on RBD and rapid evolution of SARS-CoV-2 have been reported and they could attenuate the binding as well as the antiviral activity of 5,6-DHF (Cosar et al., 2022; Wang et al., 2024), thus the activities of 5,6-DHF on binding to different RBD mutants and inhibiting current circulating SARS-CoV-2 variant such as Omicron variant JN.1 require extensive exploration. Moreover, since 5,6-DHF predominantly targets at the viral spike protein, it can be applied in a combination with other functional agents that target different stages of viral life cycle such as 3CL pro inhibitors to achieve better therapeutic effect.

Although some therapeutic agents have been proposed to combat beta-CoVs infection, more effective and safer alternatives are unmet to ensure large-scale application. In current study, we found 5,6-DHF showed promising anti-beta-CoV activity against both SARS-CoV-2 Omicron variant EG.5.1.1 and HCoV-OC43 in microneutralization test and plaque reduction neutralization test. And the antiviral activity of 5,6-DHF against beta-CoV can last for at least 5 days. It was worth mentioning that 5,6-DHF inhibited viral replication by principally blocking viral entry through interfering the spike-ACE2 interaction. Additionally, the structure-activity study emphasized the importance of the 5,6-dyhydroxyl group at the A ring for the anti-beta-CoVs activity of flavonoids.

Our findings paved the way for studying flavonoids as anti-beta-CoV agents and further exploring the functional potential of 5,6-DHF for beta-CoV post-exposure prophylaxis in animal models and human clinical trials.

CRediT authorship contribution statement

Yujia Cao: Writing – review & editing, Writing – original draft, Visualization, Validation, Software, Methodology, Investigation, Formal analysis, Data curation, Conceptualization. **Kah Man Lai:** Writing – review & editing, Writing – original draft, Validation, Methodology, Investigation. **Hongling Zheng:** Writing – original draft, Software, Methodology, Investigation, Formal analysis. **Yee Joo Tan:** Writing – review & editing, Validation, Supervision, Project administration, Methodology, Funding acquisition. **Dejian Huang:** Writing – review & editing, Validation, Supervision, Project administration, Methodology, Funding acquisition, Conceptualization.

Declaration of competing interest

The authors declare that they have no known competing financial interests or personal relationships that could have appeared to influence the work reported in this paper.

Acknowledgment

The Ministry of Education (Singapore) provided financial supports to this project by offering scholarships and a grant (A-80008417–01–00) to Yujia Cao and Hongling Zheng, and a Tier 2 funding (grant no: T2EP30121–0012) to support Kah Man Lai and consumables for virus work. We also thank Promega for preferential reagent pricing provided under the Promega Academic Access Programme.

Supplementary materials

Supplementary material associated with this article can be found, in the online version, at doi:10.1016/j.virusres.2025.199578.

Data availability

Data will be made available on request.

References

Alzaabi, M.M., Hamdy, R., Ashmawy, N.S., Hamoda, A.M., Alkhayat, F., Khademi, N.N., Al Joud, S.M.A., El-Keblawy, A.A., Soliman, S.S.M., 2022. Flavonoids are promising safe therapy against COVID-19. Phytochem. Rev. 21, 291–312.
Amanat, F., White, K.M., Miorin, L., Strohmeier, S., McMahon, M., Meade, P., Liu, W.C., Albrecht, R.A., Simon, V., Martinez-Sobrido, L., 2020. An in vitro microneutralization assay for SARS-CoV-2 serology and drug screening. Curr. Protoc. Microbiol. 58, e108.
Bader, M.S., McKINSEY, D.S., 2013. Postexposure prophylaxis for common infectious diseases. Am. Fam. Physician 88 (1), 25–32.
Chang, L., Yan, Y., Wang, L., 2020. Coronavirus disease 2019: coronaviruses and blood safety. Transfus. Med. Rev. 34, 75–80.
Cosar, B., Karagulleoglu, Z.Y., Unal, S., Ince, A.T., Uncuoglu, D.B., Tuncer, G., Kilinc, B. R., Ozkan, Y.E., Ozkoc, H.C., Demir, I.N., Eker, A., Karagoz, F., Simsek, S.Y., Yasar, B., Pala, M., Demir, A., Atak, I.N., Mendi, A.H., Bengi, V.U., Cengiz Seval, G., Gunes Altuntas, E., Kilic, P., Demir-Dora, D., 2022. SARS-CoV-2 mutations and their viral variants. Cytokine Growth Factor Rev. 63, 10–22.
da Silva, S.J.R., 2022. The emergence of new SARS-CoV-2 omicron subvariants introduces uncertainty about the end of the COVID-19 pandemic. Front Med. (Lausanne) 9, 1010489.
Dong, M., Galvan Achi, J.M., Du, R., Rong, L., Cui, Q., 2024. Development of SARS-CoV-2 entry antivirals. Cell Insight 3, 100144.
Drożdżal, S., Rosik, J., Lechowicz, K., Machaj, F., Szostak, B., Przybyciński, J., Lorzadeh, S., Kotfis, K., Ghavami, S., Łos, M.J., 2021. An update on drugs with therapeutic potential for SARS-CoV-2 (COVID-19) treatment. Drug Resist. Updat. 59, 100794.
Hashemian, S.M.R., Sheida, A., Taghizadieh, M., Memar, M.Y., Hamblin, M.R., Baghi, H. B., Nahand, J.S., Asemi, Z., Mirzaei, H., 2023. Paxlovid (Nirmatrelvir/Ritonavir): a new approach to Covid-19 therapy? Biomed. Pharmacother. 162, 114367.
He, F., Deng, Y., Li, W., 2020. Coronavirus disease 2019: what we know? J. Med. Virol. 92, 719–725.
Jantan, I., Arshad, L., Septama, A.W., Haque, M.A., Mohamed-Hussein, Z.A., Govender, N.T., 2023. Antiviral effects of phytochemicals against severe acute respiratory syndrome coronavirus 2 and their mechanisms of action: a review. Phytother. Res. 37, 1036–1056.
Kaul, R., Paul, P., Kumar, S., Büsselberg, D., Dwivedi, V.D., Chaari, A., 2021. Promising antiviral activities of natural flavonoids against SARS-CoV-2 targets: systematic review. Int. J. Mol. Sci. 22, 11069.
Lam, J.H., Khan, A.K., Cornell, T.A., Chia, T.W., Dress, R.J., Yeow, W.W.W., Mohd-Ismail, N.K., Venkataraman, S., Ng, K.T., Tan, Y.J., Anderson, D.E., Ginhoux, F., Nallani, M., 2021. Polymersomes as stable nanocarriers for a highly immunogenic and durable SARS-CoV-2 spike protein subunit vaccine. ACS. Nano 15, 15754–15770.
Li, J., Wang, Y., Solanki, K., Atre, R., Lavrijsen, M., Pan, Q., Baig, M.S., Li, P., 2023. Nirmatrelvir exerts distinct antiviral potency against different human coronaviruses. Antiviral Res. 211, 105555.
Lip, K.-M., Shen, S., Yang, X., Keng, C.-T., Zhang, A., Oh, H.-L.J., Li, Z.-H., Hwang, L.-A., Chou, C.-F., Fielding, B.C., 2006. Monoclonal antibodies targeting the HR2 domain and the region immediately upstream of the HR2 of the S protein neutralize in vitro infection of severe acute respiratory syndrome coronavirus. J. Virol. 80, 941–950.
Liskova, A., Samec, M., Koklesova, L., Samuel, S.M., Zhai, K., Al-Ishaq, R.K., Abotaleb, M., Nosal, V., Kajo, K., Ashrafizadeh, M., Zarrabi, A., Brockmueller, A., Shakibaei, M., Sabaka, P., Mozos, I., Ullrich, D., Prosecky, R., La Rocca, G., Caprnda, M., Büsselberg, D., Rodrigo, L., Kruzliak, P., Kubatka, P., 2021. Flavonoids against the SARS-CoV-2 induced inflammatory storm. Biomed. Pharmacother. 138, 111430.
Liu, H., Ye, F., Sun, Q., Liang, H., Li, C., Li, S., Lu, R., Huang, B., Tan, W., Lai, L., 2021. Scutellaria baicalensis extract and baicalein inhibit replication of SARS-CoV-2 and its 3C-like protease in vitro. J. Enzyme Inhib. Med. Chem. 36, 497–503.
Liu, L., Wen, K., Li, J., Hu, D., Huang, Y., Qiu, L., Cai, J., Che, X., 2012. Comparison of plaque-and enzyme-linked immunospot-based assays to measure the neutralizing activities of monoclonal antibodies specific to domain III of dengue virus envelope protein. Clin. Vaccine Immunol. 19, 73–78.
Liu, W., Huang, Z., Xiao, J., Wu, Y., Xia, N., Yuan, Q., 2024. Evolution of the SARS-CoV-2 omicron variants: genetic impact on viral fitness. Viruses. 16.
Markov, P.V., Ghafari, M., Beer, M., Lythgoe, K., Simmonds, P., Stilianakis, N.I., Katzourakis, A., 2023. The evolution of SARS-CoV-2. Nat. Rev. Microbiol. 21, 361–379.
Mori, M., Quaglio, D., Calcaterra, A., Ghirga, F., Sorrentino, L., Cammarone, S., Criscuolo, E., 2023. Natural flavonoid derivatives have pan-coronavirus antiviral activity. Microorganisms. 11 (2), 314.
Shmuelian, Z., Warszawer, Y., Or, O., Arbel-Alon, S., Giladi, H., Avgil Tsadok, M., Hoshen, M., 2023. Postexposure-vaccine-prophylaxis against COVID-19. J. Med. Virol. 95 (1), e28274.
Song, J., Zhang, L., Xu, Y., Yang, D., Yang, S., Zhang, W., Wang, J., Tian, S., Yang, S., Yuan, T., 2021. The comprehensive study on the therapeutic effects of baicalein for the treatment of COVID-19 in vivo and in vitro. Biomed. Pharmacother. 183, 114302.
Su, H.-x., Yao, S., Zhao, W.-f., Li, M.-j., Liu, J., Shang, W.-j., Xie, H., Ke, C.-q., Hu, H.-c., Gao, M.-n., 2020. Anti-SARS-CoV-2 activities in vitro of Shuanghuanglian preparations and bioactive ingredients. Acta Pharmacol. Sin. 41, 1167–1177.
Walle, T., 2009. Methylation of dietary flavones increases their metabolic stability and chemopreventive effects. Int. J. Mol. Sci. 10, 5002–5019.
Wang, J.F., Ding, N., Zhang, W., Wang, P., Li, Y.X., 2011. Synthesis of Ring A-modified Baicalein derivatives. Helv. Chim. Acta 94, 2221–2230.
Wang, X., Cao, Y., Chen, S., Lin, J., Yang, X., Huang, D., 2022. Structure–activity relationship (SAR) of flavones on their anti-inflammatory activity in murine macrophages in culture through the NF-κb pathway and c-src kinase receptor. J. Agric. Food Chem. 70 (28), 8788–8798.
Wang, X., Lu, L., Jiang, S., 2024. SARS-CoV-2 evolution from the BA. 2.86 to JN. 1 variants: unexpected consequences. Trends. Immunol. 45, 81–84.
Wischmeyer, P.E., Tang, H., Ren, Y., Bohannon, L., Jiang, D., Bergens, M., Sung, J.A., 2024. Efficacy of probiotic treatment as post-exposure prophylaxis for COVID-19: a double-blind, Placebo-Controlled Randomized trial. Clin. Nutr. 43 (1), 259–267.
Yadav, A., Mohite, S., 2020. A review on novel Coronavirus (COVID-19). Int. J. Pharm. Sci. Res. 11, 74–76.
Yang, J.Y., Ma, Y.X., Liu, Y., Peng, X.J., Chen, X.Z., 2023. A comprehensive review of natural flavonoids with anti-SARS-CoV-2 activity. Molecules. 28.

Zhao, T., Tang, H., Xie, L., Zheng, Y., Ma, Z., Sun, Q., Li, X., 2019. Scutellaria baicalensis Georgi.(Lamiaceae): a review of its traditional uses, botany, phytochemistry, pharmacology and toxicology. J. Pharm. Pharmacol. 71, 1353–1369.
Zheng, Z., Monteil, V.M., Maurer-Stroh, S., Yew, C.W., Leong, C., Mohd-Ismail, N.K., Cheyyatraivendran Arularasu, S., Chow, V.T.K., Lin, R.T.P., Mirazimi, .A, Hong, W., Tan, Y.J., 2020. Monoclonal antibodies for the S2 subunit of spike of SARS-CoV-1 cross-react with the newly-emerged SARS-CoV-2. Euro. Surveill. 25 (28), 2000291.
Zhu, Z., Lian, X., Su, X., Wu, W., Marraro, G.A., Zeng, Y., 2020. From SARS and MERS to COVID-19: a brief summary and comparison of severe acute respiratory infections caused by three highly pathogenic human coronaviruses. Respir. Res. 21, 224.